Applied Catalysis B: Environmental 91 (2009) 539–545

Contents lists available at ScienceDirect

Applied Catalysis B: Environmental

journal homepage: www.elsevier.com/locate/apcatb

Photoelectrochemical degradation of anti-inflammatory pharmaceuticals at Bi_2MoO_6–boron-doped diamond hybrid electrode under visible light irradiation

Xu Zhao, Jiuhui Qu *, Huijuan Liu, Zhimin Qiang, Ruiping Liu, Chengzhi Hu

State Key Laboratory of Environmental Aquatic Chemistry, Research Center for Eco-Environmental Sciences, Chinese Academy of Sciences, Beijing 100085, PR China

ARTICLE INFO

Article history:
Received 29 April 2009
Received in revised form 13 June 2009
Accepted 20 June 2009
Available online 26 June 2009

Keywords:
Ibuprofen
Naproxen
BDD electrode
Photoelectrocatalysis
Visible light

ABSTRACT

Bi_2MoO_6 particles were selectively deposited onto a boron-doped diamond (BDD) surface from amorphous complex solution via a dip-coating method followed by calcination. Its structure was confirmed via Raman and X-ray diffraction analysis. Scanning electron microscopy showed that the resulting Bi_2MoO_6 particles scattered on the BDD substrate. The photoelectrochemical measurement of the Bi_2MoO_6–BDD electrode showed a clear improvement in the photocurrent under visible light irradiation, indicating a new hybrid system. Furthermore, the hybrid electrode was applied in the degradation of ibuprofen and naproxen, two kinds of non-steroidal anti-inflammatory drugs via photocatalysis, electro-oxidation, and photoelectrocatalytic processes. It is shown that ibuprofen can be degraded via photocatalysis and electro-oxidation process with the applied bias potential of 2.0 V. By contrast, ibuprofen and naproxen can be rapidly degraded via combined electro-oxidation and photocatalysis process under visible light irradiation. Furthermore, the degradation rate in the combined process is larger than the sum of photocatalysis and electro-oxidation processes. The ibuprofen and naproxen were also efficiently mineralized in the combined process. Finally, the main intermediates of ibuprofen degradation were also identified.

1. Introduction

Photoelectrocatalysis is an efficient method in degrading organic contaminants in aqueous solution [1–5]. In the photoelectrocatalysis system, the anode is the key unit. More and more efforts have been put in developing the anode materials with high catalytic efficiency and visible light response [4,5]. Bi_2MoO_6 consisting of a layered structure with corner-shared MoO_6 units has arisen as a new visible light driven photocatalyst for O_2 evolution from an aqueous silver nitrate solution [6–8]. Its bandgap is ca. 2.70 eV and can absorb visible light with an absorbance wavelength near to 460 nm. In our previous work, Bi_2MoO_6 nanoparticles have been successfully deposited onto indium tin oxides (ITO) substrate and its photoelectrochemical properties have been investigated and the Bi_2MoO_6 film exhibit high photoelectrocatalytic activities towards degradation of dye pollutants [9].

Boron-doped diamond (BDD) electrodes have been widely investigated during the last decades because of their excellent electrochemical properties, such as: wide potential window, low background current, ultra-stability and biocompatibility, etc. [10]. The applications of BDD electrodes in electrochemical analysis, wastewater treatment and supporting catalyst have attracted many interests [11,12]. In particular, the diamond electrode has been reported to be a stable and effective electrode for environmentally oriented and analytical purposes. For example, boron doping makes it a *p*-type semiconductor as well as conductive at room temperature [13,14].

In our recent work, TiO_2 nanoparticles are selectively deposited onto the BDD film surface and TiO_2–BDD electrode exhibited high photoelectrocatalytic activities towards degrading acid orange II and 2,4-dichlorophene [15]. Thus, it is intriguing to explore the photoelectrocatalytic property of Bi_2MoO_6 on BDD which can be a better substrate for Bi_2MoO_6, in terms of efficient separation of the photoinduced charge carriers. In the present work, heterojunction films composed of Bi_2MoO_6 particles and BDD substrate were designed and fabricated. The obtained hybrid electrodes exhibit particular photoelectrochemical properties.

Human pharmaceuticals and their metabolites are discharged by sewage treatment plants to river, lake, and seawater. Numerous studies have shown that the pharmaceutical residues are widespread in the aquatic environment [16]. Ibuprofen and naproxen are kinds of the pharmaceutical drugs used for their analgesic, antipyretic, and anti-inflammatory properties [17,18]. And, they have been frequently detected in surface waters [19] and urban wastewater [20]. Their molecular structures are shown below.

* Corresponding author. Tel.: +86 10 62849151 fax: +86 10 62923558.
E-mail address: jhqu@mail.rcees.ac.cn (J. Qu).

0926-3373/$ – see front matter © 2009 Elsevier B.V. All rights reserved.
doi:10.1016/j.apcatb.2009.06.025

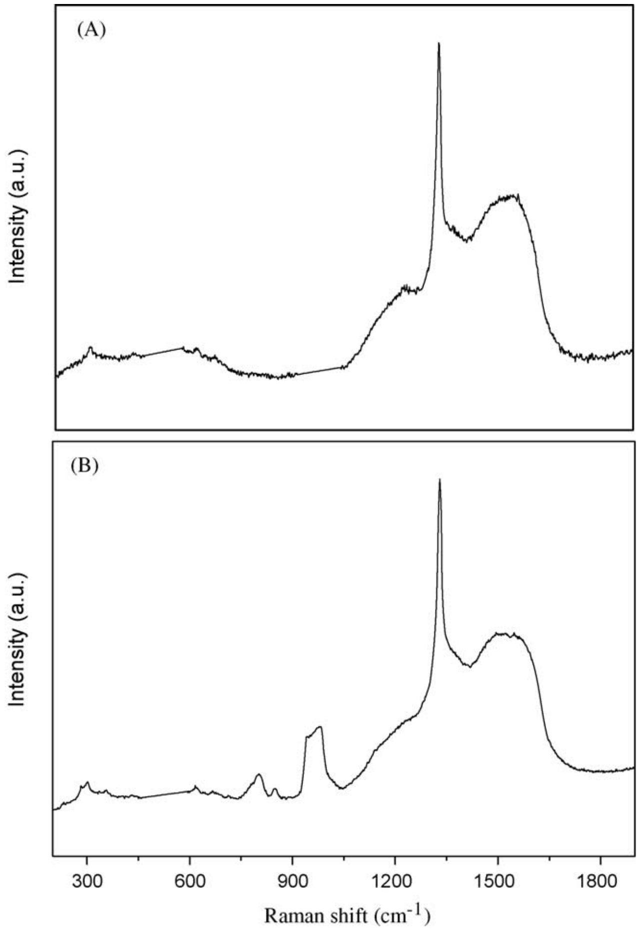

Fig. 1. Raman spectra of BDD electrode (A) and Bi_2MoO_6–BDD hybrid electrode (B).

Degradation of ibuprofen and naproxen by advanced oxidation processes such as ozonation [21–23] and UV/H_2O_2 [24] have been investigated. Photocatalysis induced by visible light irradiation, electro-oxidation, and photoelectrocatalysis degradation of ibuprofen and naproxen has not been reported. In the present work, ibuprofen and naproxen are selected as target compounds and were degraded by the prepared hybrid electrode via different processes. The obtained results indicated that the hybrid electrode showed certain photocatalytic activities towards degradation of ibuprofen and naproxen under visible light irradiation; it can also be degraded via electro-oxidation process. And a synergetic effect was observed in the degradation of ibuprofen and naproxen via combined electro-oxidation and photocatalysis process. The degradation intermediates were identified. Relatively high initial concentrations of ibuprofen and naproxen were tested in order to obtain the most plausible amount of degradation products.

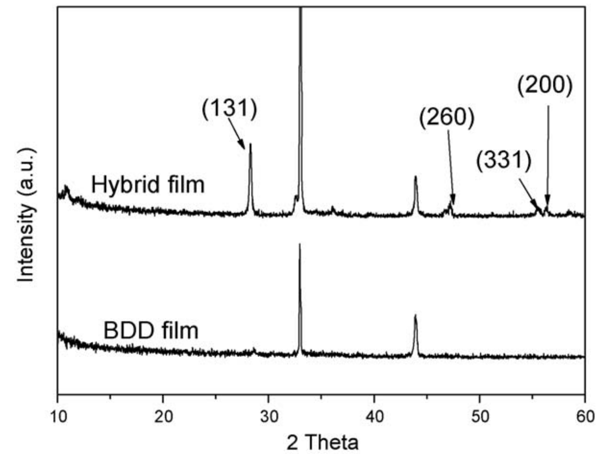

Fig. 2. XRD of BDD and Bi_2MoO_6–BDD hybrid electrodes.

2. Experimental

Ibuprofen and naproxen were purchased from Tokyo Kasei Kogyo Co., Ltd. Stock solution of ibuprofen and naproxen was prepared with Milli-Q purified water (Millipore), respectively. All chemicals used were reagent grade and were used without further purification. Highly BDD electrode used in this work were purchased from CSEM (Switzerland) and synthesized on single crystal *p*-type Si (100) wafers, with resistivity of 0.1 Ω cm, by the hot filament chemical vapor deposition technique.

Porous Bi_2MoO_6 films were deposited onto the BDD surface from an amorphous heteronuclear complex via a dip-coating method as described previously [9,25]. Raman spectra of the hybrid electrode were conducted on a Renishaw RM1000 spectrometer, the wavelength of the laser light is 514 nm. X-ray diffraction (XRD) of the Bi_2MoO_6 films was recorded on a Scintag-XDS-2000 diffractometer with Cu Kα radiation. The morphology of the Bi_2MoO_6 films was characterized by a JSM 6301 electron-scanning microscope (SEM). The photoelectrochemical measurement employed a basic electrochemical system (Princeton Applied Research) connected with a counter-electrode (Pt wire, 70 mm in length with a 0.4-mm diameter), a working electrode (the hybrid electrode, active area of 11 cm^2), and a reference electrode (a saturated calomel electrode (SCE)). 0.12 mg/L Na_2SO_4 solution was used as electrolyte solution.

Degradation experiments were performed in a cylindrical quartz reactor. The reactor, which contained a 60 mL sample solution allowing 4.5 cm of the supported film electrode to be immersed into the solution, was placed 3 cm in front of a 150 W Xe lamp purchased from the German Osram. A filter which was purchased from Shanghai Seagull Colored Optical Glass Co., Ltd. was used to remove the light with wavelength below 420 nm. The intensity of light, as measured by an irradiance meter (Instru-

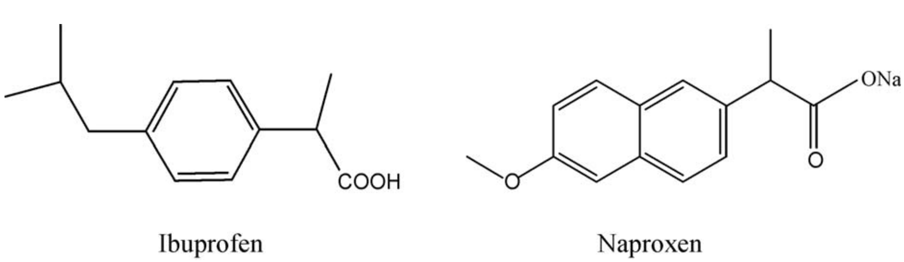

ments of Beijing Normal University) was c.a. 25 mW cm^{-2} at 4 cm into the reactor, the position where the hybrid electrode was placed. The PEC reaction employed a basic electrochemical system (Princeton Applied Research) connected with a counter-electrode (Pt wire, 70 mm in length with a 0.4-mm diameter), a working electrode (hybrid electrode, active area of 10 cm^2), and a reference electrode (SCE)). 0.1 M Na_2SO_4 solution was used as electrolyte solution. Initial concentrations of ibuprofen and naproxen solution were 10 and 15 mg/L, respectively and were analyzed by reversed phase high performance liquid chromatogram (HPLC) with a Hitachi HPLC apparatus (Diode Array Detector L-2450, C-18 column). In the case of ibuprofen, acetonitrole and 0.25 M acetic acid (75:25) were used as eluant with a flow rate of 1.0 mL min^{-1}, and the detection wavelength was set at 254 nm. In the case of naproxen, acetonitrile and 0.05 M ammonium phosphate dihydrogen (50:50) were used as eluant. And, the detection wavelength was set at 230 nm. The flow rate was also 1.0 mL min^{-1}. The concentration of total organic carbon (TOC) was analyzed using a multi N/C 3000 TOC analyzer (Analytik Jena AG, Germany). All experiments were carried out at least in duplicate. The reported values are within the experimental error of $\pm$2.9%. For gas chromatography–mass spectroscopy (GC–MS) analysis, the residue was trimethylsilylated with 0.2 mL of anhydrous pyridine, 0.1 mL of hexamethyldisilazane, and 0.05 mL of chlorotrimethylsilane at room temperature. GC–MS analysis was carried out on an Agilent 6890GC/5973MSD with a DB-5 MS capillary column. The electron spin resonance (ESR) signals of radicals spin-trapped by spin-trap reagent 5,5′-dimethyl-1-pirroline-*N*-oxide (DMPO) (purchased from Sigma Chemical Co.) were examined on a Bruker model ESR 300E spectrometer equipped with a quanta-Ray Nd:YAG laser system as the irradiation source (λ = 532 nm, 10 Hz). The $^\bullet$OH radical spin adduct of DMPO was prepared by instantaneously sampling the solution during photocatalysis, electro-oxidation, and PEC reaction with a syringe containing a constant volume of 30 mM DMPO.

3. Results and discussion

3.1. Characterization of the hybrid electrode

Fig. 1 shows the Raman spectrum of the hybrid electrode and pure BDD electrode. There is a sharp peak around 1334 cm^{-1}, slightly away from the characteristic signature of the diamond structure, 1332 cm^{-1}, revealing the presence of diamond [10]. The peak around 800 and 1000 cm^{-1} are attributed to Bi_2MoO_6 crystal [26,27]; XRD analysis of BDD and the hybrid electrode was shown in Fig. 2, the peak at 28.3θ is produced from the Bi_2MoO_6 (*JCPDS. 21–102*).

As shown in Fig. 3(A), the diamond crystals are highly faceted and have an average size of about 2 μm. A well-decorated Bi_2MoO_6 film and uniform distribution of the deposited particles on BDD compared to bare diamond was observed in Fig. 3(B). No noticeable cracks were observed on the Bi_2MoO_6 film, which ensures the high stability of the composite electrodes. As shown in Fig. 3(C), the atomic ratio of Bi to Mo is nearly 2:1, which furthermore confirms the presence of Bi_2MoO_6 at the BDD electrode surface.

3.2. Photoelectrochemical behavior of the hybrid electrode

The photoelectrochemical properties of the hybrid electrodes were examined in 0.12 mg/L Na_2SO_4 solution under visible light

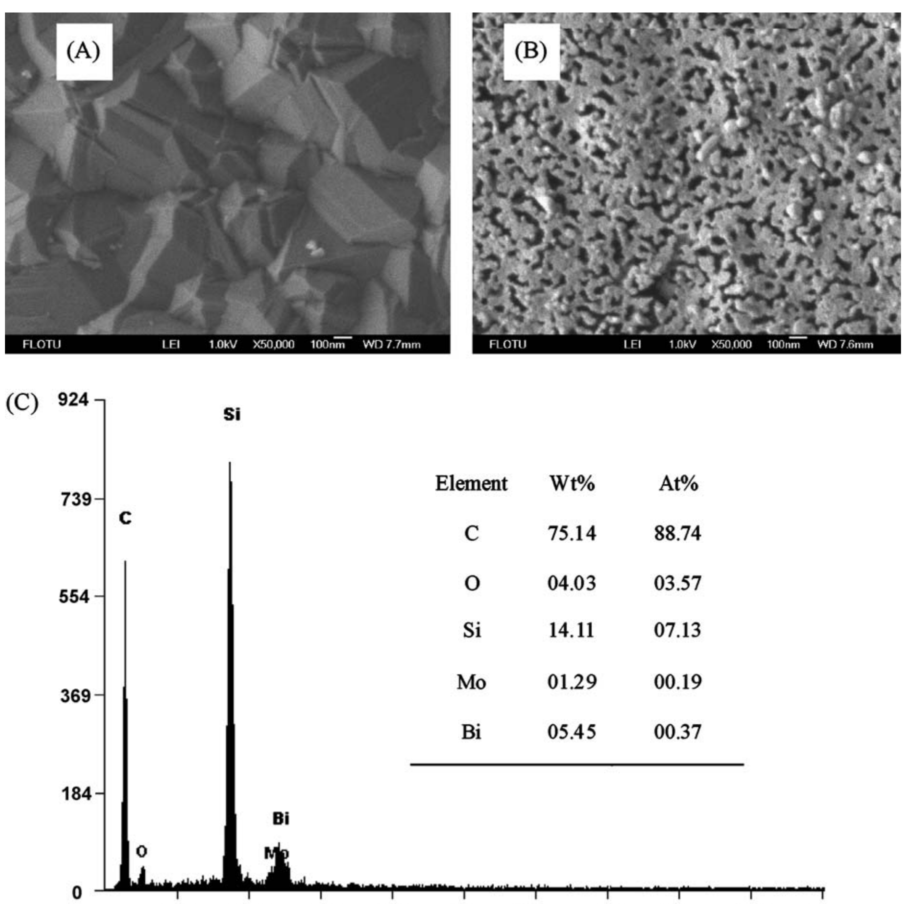

Fig. 3. SEM image of BDD (A) electrode and Bi_2MoO_6–BDD (B) hybrid electrode and energy dispersive X-ray spectroscopy (EDS) analysis (C).

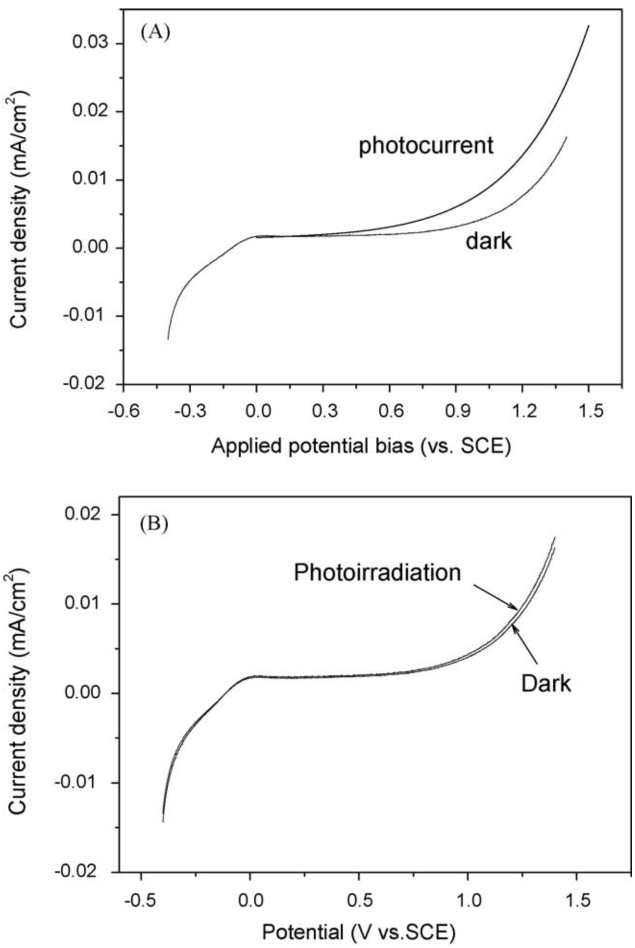

Fig. 4. Current variation of Bi_2MoO_6–BDD hybrid electrode (A) and BDD electrode (B) under dark and visible light irradiation (in 0.12 mg/L Na_2SO_4 solution, $\lambda > 420$ nm).

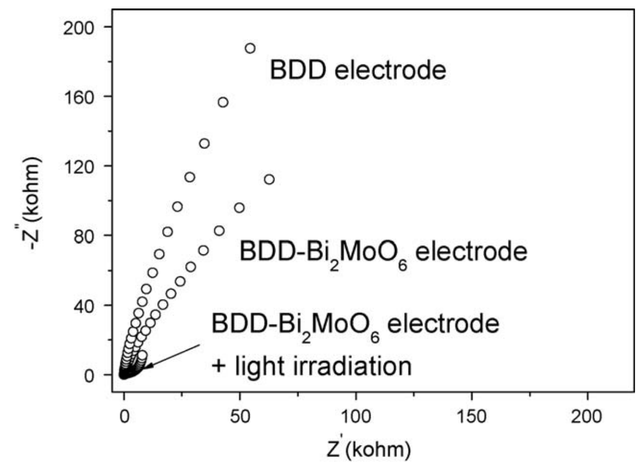

Fig. 5. EIS variation of BDD and Bi_2MoO_6–BDD hybrid electrode under dark and visible light irradiation recorded at the potential of 0 V vs. SCE (0.12 mg/L Na_2SO_4 solution).

irradiation. As shown in Fig. 4(A), photocurrent was observed for the hybrid electrode; however, no photoanode current was observed for bare BDD for the same experimental conditions (Fig. 4 (B)). Therefore, the anodic photocurrent obtained for the hybrid electrode is ascribed to the presence of Bi_2MoO_6 on BDD surface.

Typical Nyquist plots of the impedance data of the BDD electrode and hybrid electrode under dark and photoirradiation are shown in Fig. 5. It is clearly observed that the interface resistance of the hybrid electrode is lower than that of pure BDD electrode, which may be due to the heterojunction effect. Under visible light irradiation of the hybrid electrode, the size of the arc radius on the EIS Nynquist plot is largely reduced due to the photoirradiation. It is believed that the photogenerated charge carriers are efficiently utilized in this hybrid system, which furthermore confirmed the role of Bi_2MoO_6 photocatalyst in the hybrid electrode [28].

3.3. Photoelectrocatalytic degradation of ibuprofen and naproxen

It can be seen from Fig. 6(A) that the current density was increased in the presence of 10 mg/L ibuprofen at the bias potential higher than 1.0 V, which is attributed to the direct oxidation of ibuprofen at the hybrid electrode. At the bias potential higher than 1.5 V, both high current densities are observed in the presence and absence of 10 mg/L ibuprofen solution. It is suggested that O_2 was generated. Based on our previous research work, the applied bias potential of 2.0 V was selected because the hydroxyl radicals ($^{\bullet}OH$) radicals will be generated in this potential as described in our previous work [9].

As shown in Fig. 6(B), ibuprofen with 10 mg/L concentration in aqueous solution can be photocatalytically degraded at the hybrid electrode. Under visible light irradiation of the hybrid electrode, the photogenerated electron and hole can be produced from Bi_2MoO_6 particles. And, $^{\bullet}OH$ are produced, which has been reported in our previous work [9]. These active radicals are responsible for ibuprofen degradation. It can also be seen from Fig. 6(B) that ibuprofen can be efficiently degraded via the electro-oxidation process at the hybrid electrode at the bias potential of 2.0 V. Clearly, the degradation rate of ibuprofen was the largest under PEC process with the same bias potential. In PEC process, ibuprofen can be photocatalytically degraded; On the other hand, ibuprofen can also be degraded via electro-oxidation process with the applied bias potential of 2.0 V. It is known that $^{\bullet}OH$ will be produced via H_2O electrolysis reaction at the hybrid electrode. And, the synergetic effect will occur in the PEC process [29]. All of these processes are responsible for the rapid degradation of ibuprofen. At the meantime, at BDD anode with same active area, electro-oxidation degradation of ibuprofen was performed with and without visible light irradiation under same experimental conditions. Nearly no difference was observed with and without visible light irradiation (data not shown). These results confirmed the photocatalysis of Bi_2MoO_6 particles at BDD surface. Furthermore, the TOC variations in the photocatalysis, electro-oxidation, and PEC process are measured and compared. As shown in Fig. 6 (C), the TOC removal rate in PEC process is the largest in comparison with the photocatalysis and electro-oxidation process. The removal rate at the same reaction time in PEC process is larger than the sum of that in photocatalysis and electro-oxidation process. Thus, a synergetic effect was confirmed, which is consistent with the results in Fig. 6(B). The typical HPLC spectrum in PEC process was presented in Fig. 6 (D). It can be seen that with the decrease of ibuprofen peak, a peak with retention time of 5.8 min was observed. And, its intensity increases with the reaction proceeds. Subsequently, the peak intensity decreases. These results indicated that some intermediates were produced in the initial reaction phase, which were gradually degraded. At the meantime, production of $^{\bullet}OH$ was examined. As shown in Fig. 7, four characteristic peaks of DMPO–$^{\bullet}OH$ were observed in the photocatalysis, electro-oxidation, and PEC process with the applied bias potential of 2.0 V and visible light irradiation. These results indicated that $^{\bullet}OH$ radicals are produced on the surface of the hybrid film electrode in the photocatalysis, electro-oxidation, and

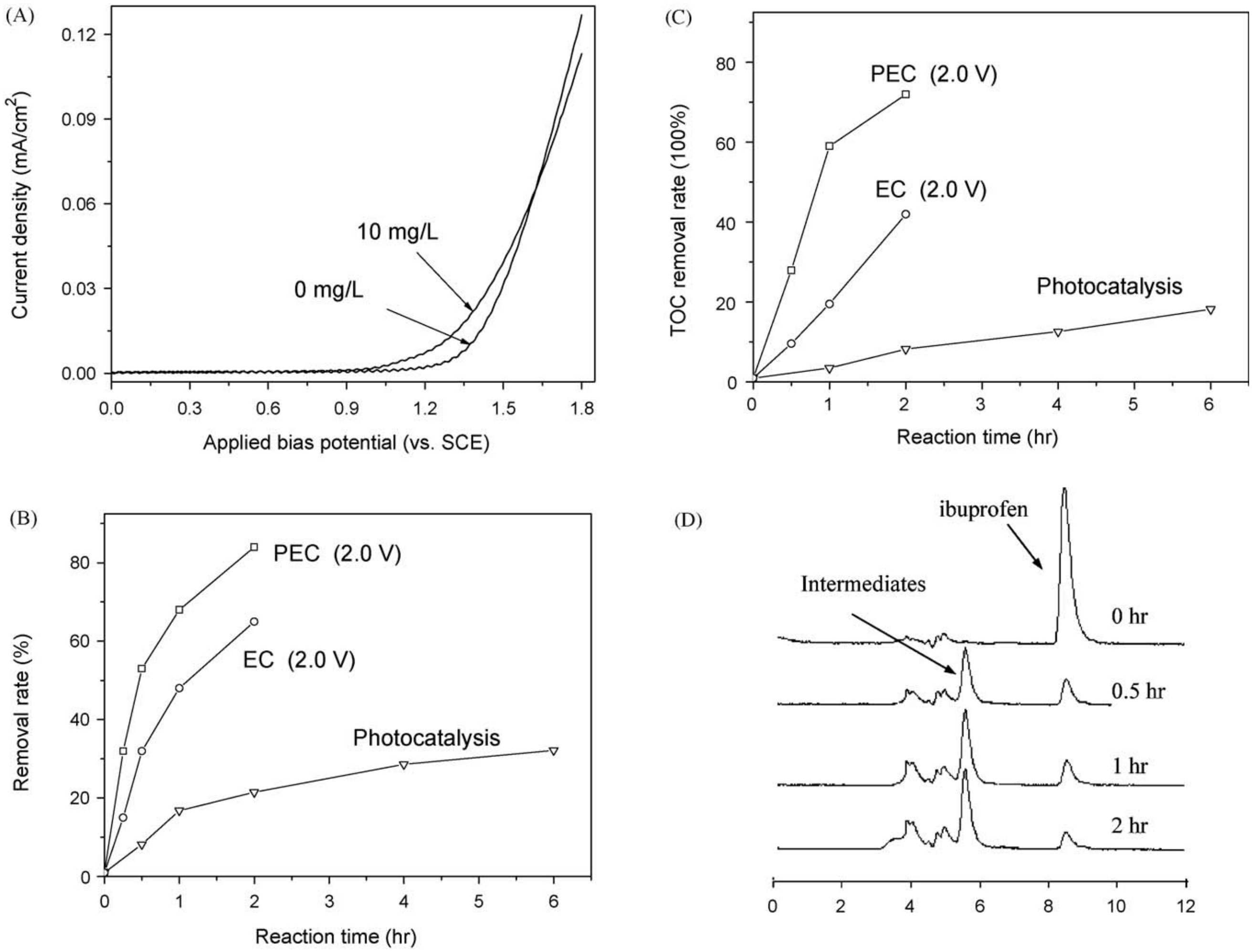

Fig. 6. Linear sweep curves of hybrid electrode aqueous solution (0.1 M Na_2SO_4 electrolyte) (A); variation of ibuprofen concentrations in the photoelectrocatalysis, electro-oxidation, and photocatalysis processes (B); TOC removal rates in the photoelectrocatalysis, electro-oxidation, and photocatalysis processes (C); HPLC spectrum variation in the photoelectrocatalysis process (D) (applied bias potential, 2 V; visible light irradiation; 0.1 M Na_2SO_4 solution).

Table 1
Main intermediates of the ibuprofen degradation in the PEC process detected by GC–MS.

Retention time min^{-1}	Intermediates	Molecular structure
8.23	2-Hydroxyl–propanoic acid	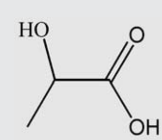
8.90	Hydroxyl–acetic acid	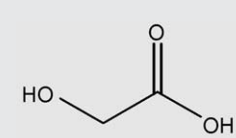
11.38	Pentanoic acid	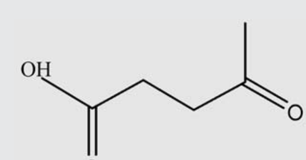

Table 1 (*Continued*)

Retention time min^{-1}	Intermediates	Molecular structure
14.82	Malonate	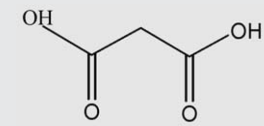
15.81	Phenol	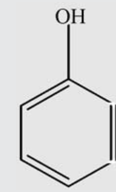
33.50	1,4-Benzenecarboxylic acid	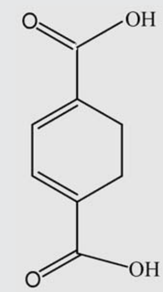

PEC process with the application of 2 V bias potential under visible light irradiation. It can also be seen that the peak intensity in PEC process is larger than that in photocatalysis and electro-oxidation process, which are responsible for the synergetic degradation of the target organic pollutants.

It was seen from Fig. 8 that naproxen can also be efficiently degraded in PEC process with the applied bias potential of 2.0 V under visible light irradiation. And, with the initial concentration of 15 mg/L, 85% naproxen was removed with a mineralization degree of 78% within 6 h. It is clear that the degradation rate of naproxen was slower than that of ibuprofen, which may be its complex molecular structure. However, the single electro-oxidation and photocatalytic degradation of naproxen was slow. Furthermore, the linear sweep of naproxen solution with the hybrid electrode was analyzed. As shown in Fig. 9, the anodic peaks at around 1.0 V appear and the peak intensity increases with the increase of naproxen concentration. These results indicate that the peak is resulting from the direct oxidation of naproxen. Therefore, the applied bias potential of 2.0 V was also selected in PEC degradation of naproxen in aqueous solution.

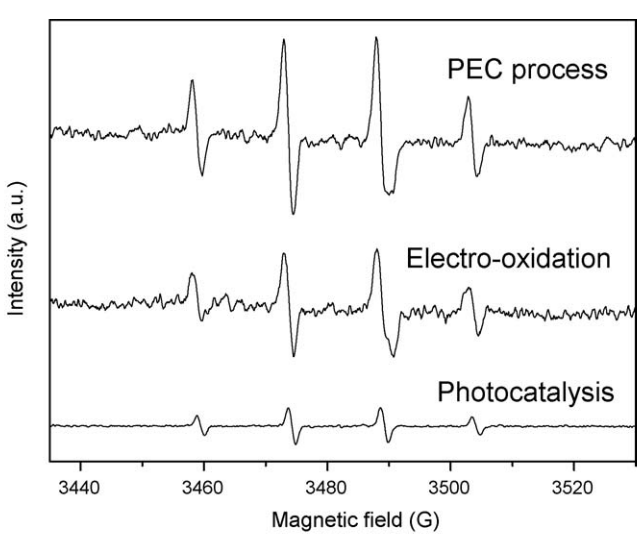

Fig. 7. DMPO spin-trapping ESR spectra recorded at ambient temperature under photocatalysis, electro-oxidation, and PEC process (the applied potential bias = 2.0 V, visible light irradiation).

For PEC process of ibuprofen, reaction samples treated at 4 h were analyzed by GC–MS. All the identified compounds were unequivocally identified using the NIST98 library database with fit values higher than 90%. Table 1 shows the intermediates detected by GC–MS from PEC treatment. Phenol and 1,4-benzenecarboxylic acid are detected. And, small molecular acids including 2-hydroxyl–propanoic acid, hydroxyl–acetic acid, pentanoic acid, and malonate are also detected. It is suggested that the probable degradation of ibuprofen is due to the $^{\bullet}OH$ mediated process. As a result, some phenol compounds were produced. Furthermore, the aromatic rings in the phenol structure were cleaved. Thus, some small molecular acids were produced. These results suggest that PEC degradation of ibuprofen proceeds by opening of phenyl ring to form small molecular organic acids. It is reported that the TiO_2 photocatalytic degradation of ibuprofen is only an early transformation process going through hydroxylated by-products, but complete mineralization is not observed. And, a direct attack on the carboxylic moiety is not observed [30,31]. Thus, it is suggested that the degradation process of ibuprofen in our PEC process using hybrid electrode is different from that in the TiO_2 photocatalytic process. At the meantime, the degradation products of naproxen in PEC process were also investigated. Some small molecular acids including butanedioic acid, acetic acid, et al were detected, which indicated that the naproxen was efficiently degraded at the hybrid electrode in PEC process under visible light irradiation.

The stability of the hybrid electrode was further investigated by repeating the ibuprofen PEC degradation experiments at the bias potential of 2.0 V for 2 h for eight times. The degradation

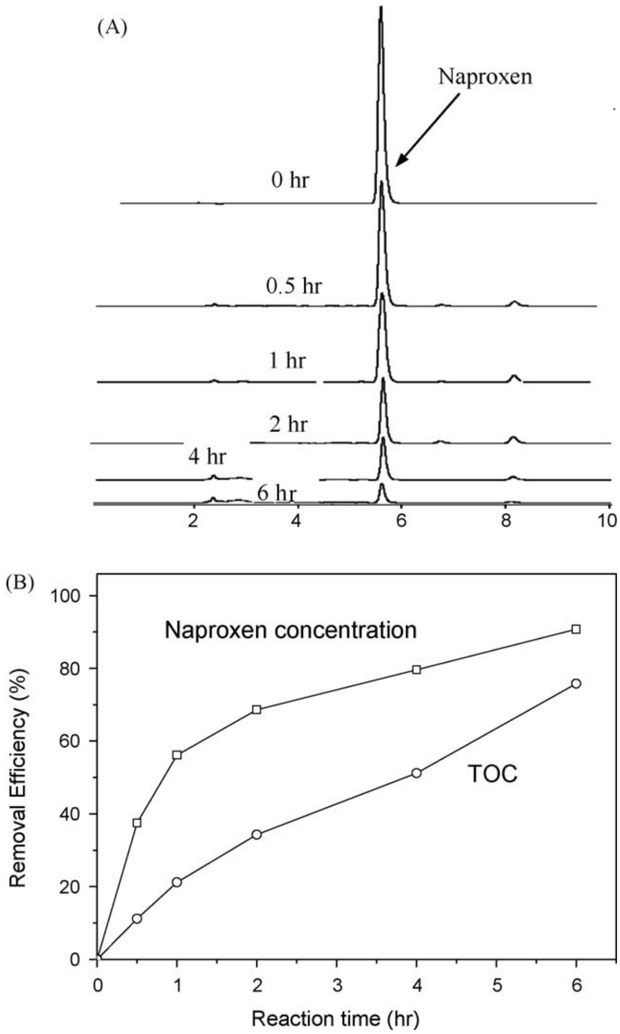

Fig. 8. HPLC spectrum variation (A) of naproxen solution and naproxen removal rate (B) in the PEC process (applied bias potential, 2 V; visible light irradiation; 0.1 M Na_2SO_4 solution).

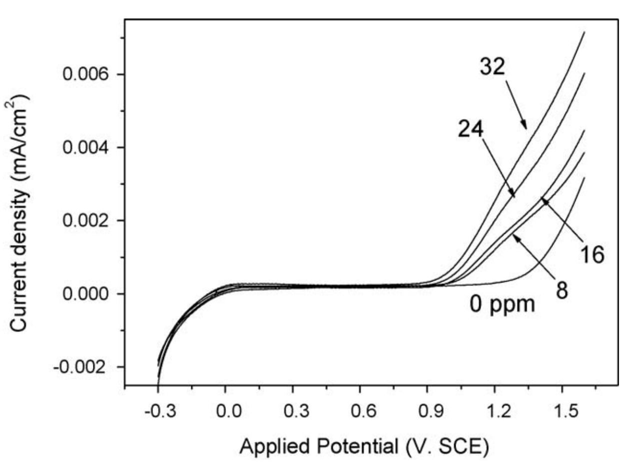

Fig. 9. Linear sweep curve of naproxen solution with various naproxen concentrations at Bi_2MoO_6–BDD hybrid electrode (0.1 M Na_2SO_4 solution).

efficiencies were ca. 82% in all the cases with the relative standard deviation of 4.2%, indicating the stability of the hybrid electrode.

4. Conclusions

The Bi_2MoO_6–BDD hybrid electrode has been fabricated and showed the expected electrochemical and photoelectrochemical activity representing the *n*-type semiconducting nature of Bi_2MoO_6. It has shown that ibuprofen and naproxen can be degraded via photoelectrocatalytic process under visible light irradiation. Their degradation rates in the combined process are larger than the sum of photocatalysis and electro-oxidation processes. The ibuprofen and naproxen were also efficiently mineralized in the combined process. The photoelectrocatalytic degradation of ibuprofen proceeded by opening of phenyl ring to form small molecular organic acids.

Acknowledgements

This work was supported by the Funds of National Natural Science Foundation of PR China (20837001, 50538090, and 50778172) and by Creative Research Groups of PR China (50621804).

References

[1] D.H. Kim, M.A. Anderson, Environ. Sci. Technol. 28 (1994) 479–483.
[2] X.Z. Li, H.L. Liu, P.T. Yue, Y.P. Sun, Environ. Sci. Technol. 34 (2000) 4401–4406.
[3] X. Quan, S. Yang, X. Ruan, H. Zhao, Environ. Sci. Technol. 39 (10) (2005) 3770–3775.
[4] L. Li, X. Zhang, Z. Ai, F. Jia, L. Zhang, L.L. Lin, J. Phys. Chem. C 111 (2007) 6832–6836.
[5] H.B. Yu, X. Quan, Y. Zhang, N. Ma, S. Chen, H.M. Zhao, Langmuir 24 (2008) 7599–7604.
[6] Y. Shimodaira, H. Kato, H. Kobayashi, A. Kudo, J. Phys. Chem. B 110 (2006) 17790–17797.
[7] J.H. Bi, L. Wu, J. Li, Z.H. Li, X.X. Wang, X.Z. Fu, Acta Materialia 55 (2007) 4699–4705.
[8] C. Belver, C. Adan, M. Fernandez-Garcia, Catal. Today 143 (2009) 274–281.
[9] X. Zhao, J.H. Qu, H. Liu, C. Hu, Environ. Sci. Technol. 41 (2007) 6802–6807.
[10] F. Beck, W. Kaiser, H. Krohn, Electrochim. Acta 45 (2000) 4691–4695.
[11] J. Iniesta, P.A. Michaud, M. Panizza, G. Cerisola, A. Aldaz, C. Comninellis, Electrochim. Acta 46 (2001) 3573–3578.
[12] X.M. Chen, G.H. Chen, F. Gao, P.L. Yue, Environ. Sci. Technol. 37 (2003) 5021–5026.
[13] O. Chailapakul, E. Popa, H. Tai, B.V. Sarada, D.A. Tryk, A. Fujishima, Electrochem. Commun. 2 (2000) 422–426.
[14] N.S.A. Manivannan, K. Arihara, A. Fujishima, Electrochem. Solid-State Lett. 8 (2005) C138–C140.
[15] J.H. Qu, X. Zhao, Environ. Sci. Technol. 42 (2008) 4934–4939.
[16] K. Fent, A.A. Weston, D. Caminada, Aquat. Toxicol. 78 (2006) 207–1207.
[17] M. Winkler, J.R. Lawrence, T.R. Neu, Water Res. 35 (2001) 3197–3205.
[18] G.R. Boyd, S.Y. Zhang, D.A. Grimm, Water Res. 39 (2005) 668–676.
[19] C. Tixier, H.P. Singer, S. Oellers, S.R. Muller, Environ. Sci. Technol. 37 (2003) 1061–1068.
[20] V. Matamoros, C. Arias, H. Brix, J.M. Bayona, Environ. Sci. Technol. 41 (2007) 8171–8177.
[21] M.M. Huber, S. Canonica, G.Y. Park, U. von Gunten, Environ. Sci. Technol. 37 (2003) 1016–1024.
[22] C. Zwiener, F.H. Frimmel, Water Res. 34 (2000) 1881–1885.
[23] F. Mdez-Arriaga, S. Esplugas, J. Gimez, Water Res. 42 (2008) 585–594.
[24] D. Vogna, R. Marotta, A. Napolitano, R. Andreozzi, M. d'Ischia, Water Res. 38 (2004) 414–422.
[25] X. Zhao, W.Q. Yao, Y. Wu, S.C. Zhang, H. Yang, Y.F. Zhu, J. Solid State Chem. 179 (2006) 2562–2570.
[26] R. Murugan, R. Gangadharan, J. Kalaiselvi, S. Sukumar, B. Palanivel, S. Mohan. J. Phys.: Condens. Matter 14 (2002) 4001–4010.
[27] F.D. Hardcastle, I.E. Wachs, J. Phys. Chem. 95 (1991) 10763–10772.
[28] W.H. Leng, Z. Zhang, J.Q. Zhang, C.N. Cao, J. Phys. Chem. B 109 (2005) 15008–15023.
[29] X. Zhao, Y. Zhu, Environ. Sci. Technol. 40 (2006) 3367–3372.
[30] J.B. Quintana, S. Weiss, T. Reemtsma, Water Res. 39 (2005) 2654–2664.
[31] G. Caviglioli, P. Valeria, P. Brunella, C. Sergio, A. Attilia, B. Gaetano, J. Pharm. Biomed. Anal. 30 (2002) 499–509.